WOODS HOLE OCEANOGRAPHIC INSTITUTION

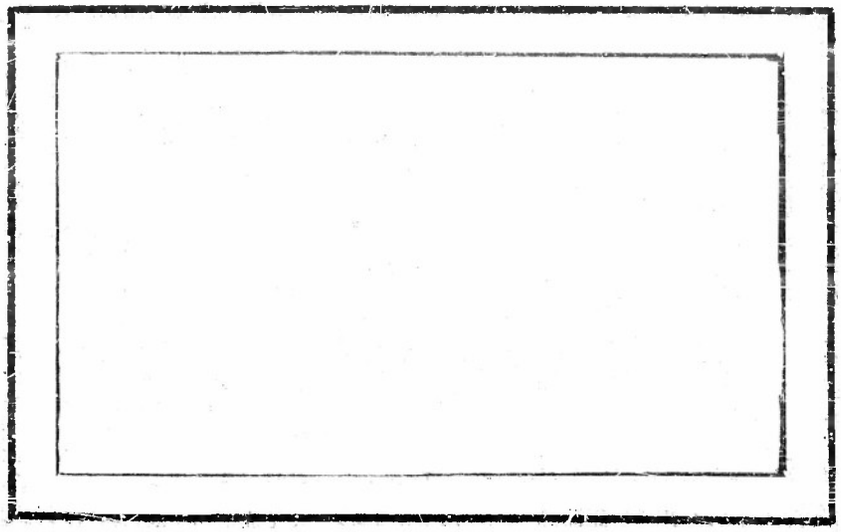

WOODS HOLE, MASSACHUSETTS

WOODS HOLE OCEANOGRAPHIC INSTITUTION

Woods Hole, Massachusetts

Reference No. 54-43

MARINE METEOROLOGY

An Example of an Orographic-Convection Cell in the Trade-Wind Region

By
Joanne Starr Malkus

Technical Report No. 30
Submitted to the Office of Naval Research
Under Contract N6Onr-27702 (NR-082-021)

June 1954

APPROVED FOR DISTRIBUTION _____
Director

Abstract

A series of four helical aircraft soundings across the island of Puerto Rico on a sea-breeze day are analyzed and interpreted. The observations give the height distribution of temperature, moisture, and small-scale turbulence at four verticals along the air flow, together with cloud observations which were supplemented by photography. The existence of a fairly symmetrical orographic-convection cell with ascent over the island and compensating subsidence in a surrounding ring is established. The field of motion in the convection cell is deduced from the observations together with the theoretical work on flow over heated islands by Malkus and Stern (1953). The plausibility of the motion field is then tested by construction of a moisture budget for part of the cross section delineated by the soundings.

I. INTRODUCTION

Although the diurnal variations in a trade-wind air mass over ocean are extremely slight, the presence of an island or land body introduces marked changes from night to day. The alteration in cloud patterns are particularly striking. Over Puerto Rico and even the smaller Virgin Islands the build-up of land and orographic clouds during the morning is commonly accompanied by clearing at the coastlines and the formation of a clear ring surrounding the island. Except in the localities where the land-formed clouds may extend seaward in a "street", the cloud-free ring extends off shore with a radius comparable to the island width. In the late afternoon as diurnal convection subsides, the clear ring shrinks again and the trade cumuli, held away during the day, are again permitted to drift inland. This sequence, common to relatively undisturbed trade regimes suggests a simple orographic-convection cell, with ascending motion over the heated land and mountains, and compensating subsidence over the coastal waters. With this picture in mind, Riehl (1947) undertook an interpretation of diurnal moisture and rainfall patterns at San Juan, Puerto Rico. His work was handicapped, however, by being confined to the use of sounding observations for the coastal region only. In Hawaii, more complicated patterns of interaction between island convection and trade winds have been studied by Leopold (1949).

Since the work of Leopold and Riehl, an extensive theoretical study of the flow of a slightly stable air stream over a heated island has been

carried out by Malkus and Stern (1953; see also Stern and Malkus, 1953; Stern, 1954). These theoretical results, coupled with the relatively simple shape and orography of Puerto Rico, suggested a more detailed study of the convection pattern produced by that island. Such a study, carried out on June 25, 1952, forms the subject of this paper. The basic data consist of a series of helical soundings performed by a slow-flying aircraft and oriented approximately parallel to the low-level wind flow. The location of the soundings relative to the island and cloud formations is illustrated on the map in Figure 1. Figures 2-5 depict the cloud configurations. The first sounding was made about 50 km east-northeast of the windward coast, in undisturbed oceanic trade-wind air. The second was made in the clear ring just off the windward shore, the third over the foothills where island convection was active, and the fourth near the seaward edge of the wider clear ring to the lee (west-southwest) of the island. One of the primary reasons for performing these observations was to study the effects of processes such as divergence, subsidence, turbulence, heating, and their opposites upon the various layers of the undisturbed trade-wind atmosphere, and upon the structure and height of the trade inversion. In an analysis of the Pacific Trade (Riehl, Yeh, Malkus, and LaSeur, 1951) budgets of moisture, momentum, and heat were calculated along a section of the flow about 2500 km in length. This was a mean picture, averaged over a two months series of observations. The latter study especially brought out the role of subsidence in creating and strengthening the trade-wind inversion and the counter-working role of

cumulus convection in raising and weakening it. In the present cross section, just over 200 km in length, the air is first subjected to subsidence (windward clear ring), then to violent turbulence, convection, and heating (over island and mountains) and then again to subsidence (leeward clear ring). It is thus possible to isolate some of these processes, working very strongly on this smaller scale, and analyze their effects separately. If by use of the theoretical work on flow over heated islands, it is possible to estimate the mean field of convective motions, a semi-quantitative budget study may be possible with these soundings. Therefore, after a discussion of the methods of measurement and the gross features of the results, the velocity field is deduced, and using it, a moisture budget attempted for a part of the cross section.

II. METHODS AND TECHNIQUES OF MEASUREMENT

The basic instrumentation of the sounding aircraft was a modified form of the M.I.T. psychrograph, described previously by McCasland (1951). The plane was flown in helical ascents of about two miles diameter at a sufficiently slow rate of climb (200 ft/min) so that lag-free values of temperature and moisture content were obtained at about 30-meter height intervals. The soundings are thus well suited to accurate determination of vertical gradients of these properties. A water column accelerometer was operated during the ascents, in order to determine the relative development of small-scale turbulence. This has been described by a parameter called the "turbulence index", defined earlier by Malkus and Bunker (1952). The

soundings in tabular form are reproduced in toto at the end of this paper. Supplementary observations included numerous still photographs (Figures 2 - 5) and wind determinations. Surface wind directions were ascertained by smoke drift and over water, smoke flares were dropped for this purpose. Winds at 1000 ft were determined by double drift, using two independent sights and observers.

The four soundings are plotted in Figure 6. Unfortunately an hour delay occurred between the end of sounding 3 and the commencement of sounding 4, due to the failure of the airplane's interphone, and sounding 4 cannot be considered synoptic with the other three. Furthermore, just as this last sounding was being made, the wind was in the process of shifting to a few degrees south of east due to the passage of a weak easterly wave.[1] Thus the trajectory of the air at the location marked 4 on Figure 1 was not along the cross section. The fact that the shift was so very recent, however, and the character of sounding 4 itself suggest that the air at that location had a significant over-island trajectory. Sounding 4 is thus included in the discussion, although the quantitative calculations are restricted to the remaining three which were performed in rapid succession between 1115 and 1415 LST.

---

[1]It may be shown by the San Juan time section that this extremely weak system produced no noticeable time-dependent effect during the observation period on the properties of the air in the cross section. Upon the aircraft's return to San Juan at 1730 LST conditions there were the same (except for the slight wind shift) as they had been early in the morning, including the height of the inversion which was checked just off shore as the plane returned to base.

III. RESULTS OF THE SOUNDINGS

The base of the trade inversion was located on each sounding and is denoted on Figure 6. It was determined by the dual criteria of a decrease in temperature lapse rate and a discontinuity in vertical moisture gradient toward more rapid drying. On soundings, 1, 2, and 4, these criteria were clearly met at the levels indicated. The inversion base possessed a mixing ratio of 8.7, 8.7, and 8.4 gm/kgm, respectively, at these locations. On sounding 3, the inversion was confused and appeared to have a multiple structure, a weak transition being indicated at 1690 m (mixing ratio 11.0 gm/kgm) and another more pronounced stabilization and drying at 2075 m (mixing ratio 8.0 gm/kgm). The soundings are more readily interpreted in conjunction with Figures 7 and 8. Figure 7 shows the distribution of potential temperature and mixing ratio in the section. Within the region delineated by the light rectangle (soundings 1 - 3) the picture may be considered synoptic and an accurate reconstruction of conditions along the air flow near noon. The remainder of the section was put together using sounding 4, theoretical calculations, other information, and speculation. The potential temperature gradient along the island surface was chosen consistent with the figures presented by Riehl (1954). He gives maximum temperatures for normal sea-breeze days at San Juan, Yayuya (elevation $\sim$600 m) and Mayaguez (lee shore). Since the sea breeze on June 25 was somewhat weaker (9 mph) than Riehl's median figure (15 mph), his maximum gradients have been toned down in Figure 7. The mountain top in the section, for example, is 6°A potentially warmer than San Juan, while Yayuya

(same elevation) often is 7 - 8°A potentially warmer on well-developed sea-breeze days. The potential temperature configuration between the lee shore (highest actual temperature, using Riehl's figures for Mayaguez) and sounding 4 was drawn consistent with the patterns off the lee shore of Nantucket observed by Malkus and Bunker (1952). The potential temperature field is everywhere consistent with the velocity field calculated and discussed later. The height to which superadiabatic and adiabatic lapse rates extend over the mountains has been governed by the height of cloud base, which in general closely delimits the top of the mixed ground layer.

Figure 8 is a schematic reconstruction of the cross section. The stabilities, cloud configurations, winds along the section at 1000 ft and inversion base are denoted thereon. The mixed ground layer is shaded. The stability is defined as $1/\theta \, d\theta/dz$, where θ is the dry potential temperature and the values plotted have been multiplied by 10^7. The average stability for each layer was obtained from the soundings by graphical averaging over each 100-meter height interval and numerical averaging of these averages over the layer in question. It was checked graphically for each layer as a whole, using Figure 6. The heights of cloud base and tops were measured, except for the tops of the clouds over the mountains, which at noon were estimated to be at about 10,000 ft. These built up to huge anvils exceeding 30,000 ft by midafternoon and died away near sundown. The operation of subsidence between soundings 1 and 2, ascent over the island, and subsidence in the leeward clear ring, indicated visually by the cloud patterns, is firmly substantiated by the stabilities and inversion behavior.

It seems profitable to discuss the effects of these processes upon each layer of the trade-wind atmosphere separately.

a. The properties of the subcloud or ground layer. - The subcloud layer is defined as the layer of air between the surface and the region of slight stabilization and drying which usually marks the cloud base. The subcloud layer exhibited by sounding 1 is typical of undisturbed oceanic trade-wind air (see Bunker, Haurwitz, Malkus, Stommel, 1949). Its depth is 575 m; it is just barely stable with respect to dry adiabatic processes; it is well-mixed and homogeneous, with a nearly constant mixing ratio. At the location of sounding 2, the character of the layer is markedly changed. It has shrunk vertically to a 450-meter thickness, stabilized by a factor of about twenty, and slightly dried (mean mixing ratio reduced by 5% compared to sounding 1). Over the plains, the lapse rate is superadiabatic up to 300 m (using the 1500 GCT San Juan sounding up to the height where the airplane sounding commenced) and adiabatic from there up to 900 m, the lowest height of a highly variable cloud base. The mean stability in the lowest 900-meter layer is negative, and the moisture uniformly distributed. Turbulence is intense and the turbulence index reached extreme values. On the last sounding at the outer edge of the leeward subsidence ring, the sub-cloud layer has shrunk again to about a 575-meter thickness, but its structure is markedly different from the normal oceanic "homogeneous" layer. The mean stability is even greater than that of sounding 2 and the average moisture lapse rate is three times greater than the undisturbed

trade-wind air at sounding 1. Most striking, however, are the intense fluctuations in mixing ratio with height, indicating that the layer was not well mixed at all, but suggesting that bunches of drier air had been brought down from aloft and not yet incorporated.

b. The relation between the structure of the subcloud layer and the initiation of cumulus growth. - Small trade cumuli uniformly based at 575 m are present at sounding 1, while clouds are entirely absent at sounding 2. Since entrainment calculations show that the lowest 300 m or so of the "cloud" layer at sounding 2 are more favorable to cumulus growth than at sounding 1, the reason for the suppression of cumuli at sounding 2 must be sought in the subcloud layer. The work of Bunker et al (1949) indicated that trade cumuli generally were found in localities where the lifting condensation level (LCL) of the lowest air fell below the top of the mixed layer, and clear spaces occurred where the LCL was more than about 30 - 50 m above its top. At sounding 1, the LCL of the lowest air is 585 m, within observational error of the top of the mixed layer and the observed cloud base. At sounding 2, the LCL of the lowest air is 560 m, which exceeds the top of the mixed layer by 110 m. That a lifting condensation level close to the top of the ground layer is not a sufficient, although a necessary, condition for trade cumulus initiation is suggested by sounding 4. No clouds appeared at sounding 4, although the LCL for the lowest air was at 600 m. Apparently the stability of the subcloud layer inhibited the upward mixing of water vapor from the sea surface and the

turbulent eddying necessary for the commencement of clouds. A few kilometers seaward of sounding 4, small cumuli based at 600 m began appearing, increasing in size still farther off shore, suggesting that the mixed layer reestablished itself and its transport functions after leaving the region influenced by subsidence.

At sounding 3 over the plains of Puerto Rico, cloud base height ranged from 900 to about 1200 m. Here the heating condensation level is probably more illuminating to calculate than the LCL. Combining the low levels of the San Juan 1500 GCT(1100 LST) radiosonde with the airplane sounding, it was found that for air with a mean mixing ratio 1 gm/kgm or 6% in excess of the sounding air, the LCL was at 900 m and no further heating was required, since the lapse rate was already adiabatic up to that level. For air with the mixing ratio of the sounding air, the HCL was at 1275 m, with 1°C rise in surface temperature required. Therefore local fluctuations over land in temperature and moisture can easily account for the observed variation in cloud base. In contrast to the oceanic trade cumuli, it appeared that the land clouds were associated with thermals extending well below their bases, since cloud-scale "bumps" could be traced under clouds down to the lowest level flown ($\sim$ 300 m).

c. The properties of the cloud layer. - The cloud layer is defined as that layer between the top of the ground layer and the base of the trade inversion, regardless of whether clouds may be actually present. Some of the most striking features of this layer on June 25 and its changes along the

section were visual. One such feature was the very great rise in cloud base, from 575 m over water to 900 - 1200 m over the plains to more than 1600 m in the mountainous area. This rise in cloud base is a characteristic feature of land vs. ocean convective clouds throughout the trade-wind region and was pronounced even over the tiny (two by ten mile) flat island of Anegada. The reasons have been clarified in the preceding sections on the subcloud layer. Second is the very different appearance of the clouds themselves (see Figures 2 - 5) for which the reasons must be sought in the properties of the cloud layer. The land and mountain clouds exhibit an appearance similar to middle-latitude clouds, with hard cauliflowerlike edges and boiling motions, in contrast to the softer, more slanting, slower overturning trade cumuli. The stability in the cloud layer is, however, far greater over the land than over the ocean, being nearly the same at soundings 1, 2, and 4, and larger by about 50% at sounding 3. This feature (namely stabilization over land in the middle and upper cloud layer) was also noted by Riehl (1947) who explained it as being due to the intense turbulence below. At the upper limit of the turbulence, a stable layer or inversion is created.

The changes along the section in the moisture structure of the cloud layer are also of interest. Between soundings 1 and 2, the average mixing ratio of the cloud layer (roughly 500 - 1500 m vertical extent) decreases by 13%. Since on soundings 3 and 4 the total thickness of the cloud layer becomes much greater, the mean mixing ratios are not comparable, but rather the differences in vapor content which may be expected between clouds and

their surroundings. The difference in mixing ratio between the sounding air and saturated air at the same temperature and pressure was taken as a measure of this. The 1500 m level was used as an example. At sounding 1 the difference was 6.2 gm/kgm; at sounding 2 it was 6.0 gm/kgm; at sounding 3, 3.3 gm/kgm; and at sounding 4, 4.4 gm/kgm. Thus over the island the greater stability in the cloud layer was far more than offset by three factors, a) strong thermals below cloud base, b) general ascent in the mean motion, and c) reduced resistance due to dry-air entrainment.

d. Features of the moist layer as a whole and of the trade inversion. - In the tropics, the moist layer is defined as the layer from the surface up to the inversion base. The moisture structure of sounding 4 clearly shows the effects of passage over the island. The moist layer extends up to 2300 m, compared to 1600 m on sounding 1. Relative to sounding 1, the air from 500 - 1300 m has dried, decreasing its mean mixing ratio by 10% and the air from 1300 - 2000 m has been moistened, increasing its mean mixing ratio by 38%. The moist layer as a whole has thus accumulated water vapor in passing from sounding 1 to sounding 4. The total precipitable water in a unit column from the sea surface to the base of the trade inversion at sounding 1 was calculated to be 2.59 gm/cm^2, while at sounding 4 it had become 3.18 gm/cm^2, an increase of 23%.

The location of the base of the trade inversion, where it was known, is given on Figure 8. Between sounding 1 and sounding 2 it sank 200 m and strengthened. Using the mean windspeed at the 1500 m level, this gives an

average subsidence rate of 0.8 cm/sec. Figure 7 shows that the potential temperature of the inversion base is conserved between those locations (about 303.4°A) and thus the inversion contour delineates the air parcel trajectories and also the streamlines if a steady state may be assumed. After the coastline is crossed, the isentropes begin crossing the inversion contours very rapidly and at sounding 4 the potential temperature of its base is nearly 308°A. Level for level compared to sounding 1, sounding 4 shows a net warming up to 1000 m, a net cooling above about 2000 m, and a marked destabilization or more nearly adiabatic lapse rate between 1000 and 2000 m, shown by the wider spacing of the isentropes on sounding 4. This is to be expected from the overturning and convection occurring over the island. The increased strength of the inversion on sounding 4, both in respect to stability and vertical rate of drying must be due to the fact that the inversion delimits the upper boundary of convection and overturning, rather than to the subsidence, which will be shown to have weakened or disappeared by 2000 m elevation.

IV. THE FIELD OF MOTION

a. The observed wind structure. - Surface smoke showed directions fluctuating between 60 - 88° on soundings 1 - 3. Double drift readings at 1000 ft in each of these locations indicated little or no shift in direction with height. The 1500 GCT radio-wind observation at San Juan showed little wind shear up to 3 km. Thus the average 1000 ft wind at soundings 1 and 4, namely 4 mps is taken as a constant basic current throughout the section,

upon which the mean convective motions are to be superposed. These are calculated in the paragraphs to follow.

b. Calculation of the mean convective motions. - It is assumed that the sea-breeze convective cell is in a nearly steady state during the hours around noon, as has been justified for smaller islands by the work of Malkus and Stern (1953).

The velocities in this cell are computed as follows: A circular island of radius 50 km is considered, with an elliptical subsidence ring around it; the subsidence ring is 40 km across on the upwind side and 80 km across on the downwind side. An inward-pointing sea breeze is taken around the coast line of 3.6 mps on the upwind coast (difference between observed winds at 1000 ft at soundings 1 and 3), increasing to 4 mps on the lee coast (due to calm at 1000 ft observed there). Inland, the sea breeze is assumed to go linearly to zero at the island center and out to sea it goes linearly to zero at the periphery of the subsidence ring. If we assume strictly radial velocities, the low-level divergence pattern is thus specified, and to complete the determination of the velocity field it is only necessary to find the height at which the sea breeze reverses. Stern and Malkus (1953) have derived an expression for this height, namely

$$h = \frac{\pi}{2} \frac{1}{\sqrt{\frac{gs}{U^2}}}$$

where U is the basic current, g is the acceleration of gravity and s is the stability of the undisturbed current. Taking U = 4 mps, and s as the mean stability of the moist layer on sounding 1, this height h comes out 850 m. Therefore, the horizontal divergence field is taken as constant from the surface to 300 m, is decreased linearly from there to zero at 900 m over the water (1000 m over the island) and increased linearly in the opposite sense up to surface magnitude at 1500 - 1800 m.

Thus $\partial w / \partial z$ and w are specified. When w is so calculated, the convective and total (4 mps basic current added) velocities along the section give the streamlines shown in Figure 9. The maximum rate of descent in the subsidence ring is 3.3 cm/sec at 900 m, and the maximum rate of ascent over the island is about 10 cm/sec at 1000 m. The rate of descent in the subsidence ring at 1500 m comes out 1.2 cm/sec in fair agreement with the 0.8 cm/sec calculated from the sinking of the inversion between soundings 1 and 2. In constructing Figure 9, the presence of the actual mountain ridge has been ignored, for although it undoubtedly disturbs the flow and adds to the circulation, the "equivalent mountain" due to the heating may be shown (see Stern and Malkus, equations 34 and 35, loc. cit.) to be at least 1 1/3 times as high as the actual 600 m mountain, provided that the average island surface temperature exceeds the sea temperature by 1.5°C. Since the temperature at the lee shore (on Figure 7) exceeds that on the windward by 4°C, thus mean temperature excess is not exaggerated, and the "equivalent mountain" amplitude of 800 m is consistent with the vertical amplitude of the streamline

flow, as also was found in the previous studies.

An independent test of the velocity field is, however, possible. The calculated motions must transport water vapor through and within the section in such a way that mass continuity is satisfied, using the mixing ratios and gradients observed on the soundings. The next section is thus concerned with the moisture balance.

V. THE MOISTURE BUDGET OF THE SECTION

Soundings 1, 2, and 3 are assumed synoptic and describing a steady-state air flow. We consider a volume 1 cm in width normal to this section (see Riehl et al, 1951). The equation of mass continuity says that the total rate of moisture influx into this volume must equal the total rate of moisture efflux. Since no precipitation was occurring in this part of the section the processes which must achieve the balance in the lowest layer are: Evaporation into the section from the sea; influx at the upstream side and efflux at the downstream side; efflux or influx along the top depending on whether subsidence or ascent is occurring in the mean convective motion; and efflux from the top due to turbulence. Symbolically we may write

$$\rho\int_0^H U_{iqi}\,dz + Ed - \overline{w}pq_H d - \rho\int_0^H U_E q_E\,dz - \int_0^d A\left(\frac{\partial q}{\partial z}\right)_H dx = 0$$

where the z - direction is vertically upward; the x - direction points along the basic flow; the section has a height H and a length d. The first term is the influx at the upstream end due to the horizontal motion along

the section, U_i; q_i is the mixing ratio at the influx end, and ρ is the air density assumed constant throughout the section. The second term is the moisture addition due to evaporation, E being the evaporation rate in $gm/cm^2 sec$. The third term is the flow through the top of the section where $\overline{w}$ is the mean vertical motion along the length of the top, and q_H is the mean mixing ratio along the top. The fourth term is the horizontal efflux at the downstream end and the last term is the efflux through the top due to turbulence. The upward gradient of moisture at the level H is $\partial q / \partial z$ and A is the Austausch or coefficient of turbulent moisture exchange. All these quantities except the evaporation rate and the Austausch are determined by the field of motion and the soundings. If the evaporation rate can be estimated, the Austausch may be calculated and a similar budget equation evolved for the next higher layer of the section. The procedure followed here is that a balance is assumed, and the Austausch calculated at several levels, first between soundings 1 and 2, and second between soundings 2 and 3. A reasonable space distribution of Austausch, while by no means a proof of the motion field, may be considered a confirmation of its plausibility, since fairly small alterations in velocities would change the Austausch distribution considerably. The process is illustrated in detail for the lowest 300-meter layer between soundings 1 and 2, and the results of the remaining calculations are shown in Figures 10 and 11. The Austausch distribution over land was found from the average Austausch between soundings 2 and 3 by extrapolating the overwater Austausch up to the coastline.

The figures for the lowest 300-meter section between soundings 1 and 2 are as follows:

Horizontal influx term = $\rho \bar{U}_i \bar{q}_i H = 10^{-3} \times 4 \times 10^2 \times 18.2 \times 10^{-3} \times 3 \times 10^4 = 219$ gm/sec

Horizontal efflux = $\rho \bar{U}_E \bar{q}_E H = 10^{-3} \times 7 \times 10^2 \times 17.8 \times 10^{-3} \times 3 \times 10^4 = 347$ gm/sec

Subsidence through top = $\rho \overline{wq}_{300} d = 10^{-3} \times 1.8 \times 17.6 \times 10^{-3} \times 50 \times 10^5 = 159$ gm/sec

Evaporation = $Ed = 8 \times 10^{-6} \times 50 \times 10^5 = 40$ gm/sec

where the evaporation rate of 8×10^{-6} gm/cm^{2}sec has been chosen, which is twice the mean annual evaporation rate for the region (Sverdrup, 1942).

Turbulent Flux = $A_{300} \left(\frac{\partial q}{\partial z} \right)_{300} d = A_{300} \times 5 \times 10^{-9} \times 50 \times 10^5$

Applying the balance equation, A_{300} comes out 176 gm cm^{-1}sec^{-1} or 200 gm cm^{-1}sec^{-1} within the errors of the calculations. The height distribution of Austausch coefficient of Figure 11 is plausible and in good agreement with values obtained for the Caribbean (Bunker et al., 1949) and in the Pacific Trade by Riehl et al. (1951). The higher values and greater vertical extent of the turbulence over land is also indicated by the much higher "turbulence index" on sounding 3 compared to the others (see tabulated data at the end of the paper).

VI CONCLUDING REMARKS

The calculated velocity field is thus quantitatively reconcilable with the observed moisture field and qualitatively reconcilable with the

inversion and potential temperature distribution. The predictions of Riehl (1947) concerning the basic features of the orographic-convection cell produced by Puerto Rico may thus be considered verified.

Among the more interesting conclusions which may be drawn from the present study concerns the sensitive balance between the processes normally operating in an undisturbed trade stream. The average interaction of these processes establishes the mean distribution of convection and diffusion, the mean height and strength of the inversion, and so forth. Especially important is the upward transport of water vapor through the subcloud and cloud layers. This upward transport of vapor has been demonstrated (see Riehl, 1954, pp. 150-153; 376-380) to be of importance to the general circulation as a whole, as well as to the rainfall and heat budgets of the tropics. The trade cumuli have been indicated as the major mechanism of this transport through a significant vertical layer, and their suppression over a significantly large area or time may not only cause local drought but a disturbing influence upon larger-scale events.

It has been shown here that small alterations in the subcloud layer due to subsidence may completely suppress the appearance of cumuli, despite little or no changes in the properties of the cloud layer itself. This is due to the very marginal condition of the normal subcloud layer. Under ordinary conditions, a decrease in lapse rate of less than $0.1^{\circ}C$ per 100 m may increase the stability by more than a factor of five; or a decrease of mixing ratio of 0.5 gm/kgm at the top of the layer may double the moisture gradient. Either of these changes greatly affects the upward

transports carried out by the eddies in the layer. Subsidence is a particularly effective suppressor of cumuli since it both stabilizes and thus damps the eddies and also may lower the top of the mixed layer below the lifting condensation level of the air within it. At higher levels, subsidence serves to lower and strengthen the trade inversion, the contours of which we see from Figure 8 would be far different without the normally observed counteraction of the cumuli.

A heated land mass produces the opposite effects. Over an island the size of Puerto Rico on even a slightly subnormal sea-breeze day, the height of cloud top is raised from an undisturbed 700 m over water to 3 km over land by noon and to more than 9 km by mid-afternoon. After leaving the island the air had experienced a net 800 m raising of the trade inversion and a 23% increased accumulation of water vapor in the moist layer. Clearly an observer's picture of the trade-wind atmosphere will depend critically upon whether he observes over water or over land, and if over land, upon the size of the land mass and his particular location with respect to it.

In conclusion, the very delicate equilibrium governing the trade-wind air stream raises the possibility of artificial attempts to alter it in limited areas. In particular, the critical condition of the subcloud layer indicates that man-made efforts to increase tropical rainfall might more fruitfully be concentrated upon the air below cloud and upwind of the islands rather than upon the already existant clouds over the region where rain is desired, which this study suggests are in a far less marginal balance.

Acknowledgments

The writer acknowledges with gratitude the large contribution made to this study by Mr. Kenneth McCasland, who suggested that the clear ring around Puerto Rico be investigated in the manner described here. He is also nearly single-handedly responsible for the instrumentation and many of the observational procedures. The photographs are the work of Mr. Claude Ronne who also participated valuably during the analysis, as did Dr. Herbert Riehl whose publications form an irreplaceable background for all trade-wind studies of this type.

The soundings were reduced and checked by Mrs. Phyllis Casiles. The drawings represent the drafting skill of Mr. Frank Bailey and are reproduced here by the care and efficiency of Mr. John Stimpson.

References

Bunker, A. F., B. Haurwitz, J. S. Malkus, and H. Stommel, 1949: Vertical distribution of temperature and humidity over the Caribbean Sea. Pap. Phys. Ocean. & Meteor., Mass. Inst. of Tech. and Woods Hole Ocean. Inst., 11, No. 1, 82 pp.

Leopold, L. B., 1949: The interaction of trade wind and sea breeze, Hawaii. J. Meteor., 6, 312-320.

Malkus, J. S. and A. F. Bunker, 1952: Observational studies of the airflow over Nantucket Island during the summer of 1950. Pap. Phys. Ocean. and Meteor. Mass. Inst. of Tech. and Woods Hole Ocean. Inst., 12, No. 2, 50 pp.

Malkus, J. S. and M. E. Stern, 1953: The flow of a stable atmosphere over a heated island, Part I. J. Meteor., 10, 30-41.

McCasland, K., 1951: Modifications of the airplane psychrograph and adaptation of the humidity strip to airplane soundings. W.H.O.I. Ref. No. 51-59. Unpublished manuscript submitted to the Office of Naval Research under Contract No. N6onr-27702 (NR-082-021). 10 pp.

Riehl, H., 1947: Diurnal variation of moisture and stability aloft in the vicinity of San Juan, Puerto Rico. Bull. Amer. Met. Soc., 28, 137-143.

Riehl, H., 1954: Tropical Meteorology. McGraw Hill Book Co., New York 392 pp.

Riehl, H., T. C. Yeh, J. S. Malkus, and N. E. LaSeur, 1951: The northeast trade of the Pacific Ocean. Quart. J. Roy. Met. Soc., 77, 598-626.

Stern, M. E., 1954: A hypothesis on atmospheric heating and its consequences in terms of the sea breeze. W.H.O.I. Ref. No. 53-8. Unpublished manuscript submitted to the Office of Naval Research under Contract No. N6onr-27702 (NR-082-021) 25 pp. In press, J. Meteor.

Stern, M. E. and J. S. Malkus, 1953: The flow of a stable atmosphere over a heated island, Part II. J. Meteor., 10, 105-120.

Sverdrup, H. U., 1942: Oceanography for Meteorologists. Prentice Hall Book Co., New York. 235 pp.

Titles for Illustrations

Fig. 1. Map showing the topography of Puerto Rico, the locations of the four soundings, and the cloud distribution (schematically) near noon on June 25, 1952. The 1000-ft contour is dashed; the 2000-ft, x-ed; the 3000-ft solid, and the 4000-ft, dotted. The light solid line through the sounding locations is the cross section constructed (see Figures 7-9); the arrows show the directions aimed by the camera in the photographs to follow (Figures 2-5). The dashed lines running from soundings 1 and 4 to shore indicate where horizontal runs were made by the observing aircraft. The latter data are omitted from the discussion since little new information was added by them.

Fig. 2. Photographs taken at location of sounding 1, 1200 LST, 6000 ft elevation.

a. Photograph of trade cumuli seaward of subsidence ring, along direction of arrow a on Figure 1.

b. Photograph of clear ring and clouds along coastal plane (over island), along direction of arrow b on Figure 1. Coastline is visible in right foreground.

Fig. 3. Photographs taken at location of sounding 2, 1333 LST, 6000 ft elevation.

a. Photograph along arrow a of coastal plane clouds. All clouds seen here are land-formed.

b. Photograph along arrow b of coastal plane clouds. Outskirts of San Juan are in right foreground.

Fig. 4. Photographs taken on way to location of sounding 4, 1436 LST, about 2000 ft elevation.

a. Photograph taken at location and in direction of arrow a showing lee coast of Puerto Rico, lee side subsidence ring, and oceanic cumulus farther to seaward.

b. Photograph taken at location and in direction of arrow b showing oceanic trade cumuli to seaward of subsidence ring off lee shore.

Fig. 5. Photographs taken at location of sounding 4, 1600 LST, 8400 ft elevation.

a. Photograph along arrow a showing coast line and cumulonimbus cloud over mountain range.

b. Photograph along arrow b showing oceanic trade cumulus to south of leeward subsidence ring.

c. Photograph taken along arrow c showing land clouds to the right, clear ring, and oceanic clouds to the left.

Fig. 6. Temperature (right-hand curves) and mixing ratio (left-hand curves) as a function of height for each of the four aircraft soundings. The values at the lowest observation point are given at the base of each curve. Each curve thus has the same scale but a different origin. Sounding 3 (over land) began at 300 m elevation

and was extrapolated down dry adiabatically and at constant mixing ratio (dashed lines).

Fig. 7. Cross section of potential temperature and mixing ratio along the line indicated on Fig. 1, near noon, June 25, 1952. The contours of Puerto Rico are shown by the hatched profile. Isentropes are solid lines; lines of constant mixing ratio are dashed. The region outside the light rectangle (soundings 1-3) is partly speculative (see text) and not used in quantitative calculations.

Fig. 8. Schematic reconstruction of the cross section shown in Fig. 7, giving the thickness of the subcloud layer (hatched); the distribution of the inversion base (solid, dashed on sounding 3), average stabilities for the layers indicated (x 10^7 cm^{-1}), cloud configurations and 1000-ft winds which were determined by double drift of the aircraft. It should be noted that the stabilities were calculated by layers and are therefore not comparable for the same height interval from one sounding to the next.

Fig. 9. Streamlines (calculated) of the air flow along the cross section of Figs. 7 and 8. The streamlines of the convection cell are dashed; the total streamlines are solid (obtained by adding constant basic wind of 4 mps from right to left).

Fig. 10. Moisture budget for the volume 1 cm normal to the section of Figs. 7-9. The numbers accompanying the arrows are moisture fluxes

in gm/sec into and out of the sub-volumes.

a. Budget for the volume 50 km in length between soundings 1 and 2, which was divided into four layers: lower subcloud (0-300 m); upper subcloud (300-500 m); cloud (500-1500 m); inversion (1500-1950 m). The turbulent transport through the 1500 and 1950 m levels was zero despite a strong rate of decrease of mixing ratio upward, thus indicating a negligible Austausch at these levels.

b. Budget for the volume 12 km in length between soundings 2 and 3, which was divided into three layers: lower subcloud, (0-500 m); upper subcloud (500-1000 m); cloud (1000-1800 m). The much shorter length of this section makes its figures rather unreliable compared to the previous one, especially since some gradients and transports (those indicated by double arrows) were averaged across the top which includes a water-land transition. Nevertheless the results are consistent with one another and with the sounding data.

Fig. 11. Austausch, or moisture exchange coefficient, as a function of height, calculated from the results of Fig. 10 taking the turbulent transport, T, and the vertical moisture gradient at the level in question. The values over land (dashed curve) are computed by obtaining the average value between soundings 2 and 3 (Fig. 10b) and extrapolating the value over water (solid curve) up to the coastline.

Table I - Sounding 1 Over ocean

1115 - 1140 LST

Height m	Pressure mb	Temperature °C	Mixing Ratio gm/kgm	Turbulence Index
35	1016	28.5	18.5	9
63	1013	28.3	18.7	10
99	1009	28.0	18.5	11
132	1005	27.6	18.0	11.5
158	1002	27.5	18.1	12
192	998	27.0	17.9	13
220	995	26.7	17.9	8
258	991	26.3	17.8	7
292	987	25.9	17.9	7.5
320	984	25.7	18.1	8
355	980	25.2	17.6	7
383	977	25.1	17.9	7
483	966	23.6	17.3	6
493	965	23.4	17.3	6
500	964	23.2	17.1	5.5
510	963	23.2	16.9	5
547	959	23.3	16.9	4
555	958	23.2	16.2	4
565	957	23.2	16.2	4
575	956	22.5	16.2	4
610	952	22.6	15.6	3
635	949	22.5	15.6	2

Table I - Sounding 1
(continued)

Height	Pressure	Temperature	Mixing Ratio	Turbulence
m	mb	°C	gm/kgm	Index
675	945	22.3	15.3	2
700	942	22.1	15.2	2
740	938	21.6	15.1	3
767	935	21.5	15.1	2.5
795	932	21.1	15.1	2
832	928	21.1	14.9	2
860	925	20.7	15.1	2
897	921	20.5	14.7	2
925	918	20.2	14.8	2
955	915	20.0	14.6	2
990	911	19.9	14.5	2
1020	908	19.8	13.5	2
1045	905	20.2	13.0	2
1085	901	19.8	12.7	2
1112	898	19.7	12.7	2
1143	895	19.8	12.4	2
1182	891	19.4	12.7	2
1212	888	19.4	11.9	2
1240	885	19.2	11.5	2.5
1260	882	18.6	12.2	3
1310	878	18.4	12.4	2.5
1340	875	18.3	11.7	2
1350	874	18.0	11.1	2

Table I - Sounding 1
(continued)

Height	Pressure	Temperature	Mixing Ratio	Turbulence
m	mb	°C	gm/kgm	Index
1370	872	18.3	9.8	2
1399	869	17.9	8.5	2
1436	865	17.7	8.4	1
1465	862	17.1	10.2	1
1495	859	17.3	8.6	1
1529	856	16.7	8.6	3
1560	853	16.7	8.1	3
1605	849	16.5	8.8	3
1640	846	16.6	8.7	3
1670	843	16.5	8.2	3
1705	840	16.9	6.1	3
1740	837	16.8	6.0	3
1770	834	16.0	6.3	3
1805	831	16.0	5.9	2.5
1639	828	16.0	6.3	2
1881	824	15.8	6.2	2
1912	821	15.9	6.0	1.5
1950	818	15.4	5.9	1

Table II - Sounding 2 In subsidence ring.

1255 - 1326 LST

Height m	Pressure mb	Temperature °C	Mixing Ratio gm/kgm	Turbulence Index
18	1018	27.7	18.4	14
36	1016	27.8	18.2	13.5
67	1012.6	27.3	18.3	13
98	1009	27.2	18.2	12
133	1005	26.8	18.15	11
166	1001.6	26.5	17.5	8
196	998	26.1	17.8	6
230	994.4	25.9	17.6	6
263	990.8	25.7	17.8	9
294	987.3	25.3	17.6	7
327	983.7	25.1	17.8	9
360	980.2	24.7	17.6	8.5
390	976.6	24.2	17.9	8
424	973	24.1	17.6	7.5
456	969.6	23.9	17.8	7
488	966	23.7	16.9	7
519	962.6	23.3	16.8	6
550	959	23.3	16.5	6
643	948.6	22.0	16.1	4
675	945	22.2	16.1	4
708	941.7	22.2	15.9	3
739	938.3	22.0	15.3	3
772	934.8	21.8	15.1	4

Table II - Sounding 2
(continued)

Height	Pressure	Temperature	Mixing Ratio	Turbulence
m	mb	°C	gm/kgm	Index
804	931.4	21.5	15.1	3
834	928.0	21.3	15.2	3
868	924.6	20.95	14.7	2
898	921.3	20.85	14.7	4
930	917.8	20.7	14.6	4
961	914.5	20.5	14.5	3
992	911.2	20.2	14.2	4
1024	907.8	20.8	12.9	5
1054	904.5	20.2	13.4	4
1086	901.2	19.9	13.7	5
1119	897.8	19.5	13.9	5
1152	894.4	19.5	13.9	5
1182	891.2	19.5	12.5	4
1213	888.0	19.2	12.7	4
1247	884.7	19.0	12.6	3
1277	881.6	19.5	11.2	4
1310	878.2	19.0	11.5	3
1341	875.0	18.6	11.2	2
1374	871.7	18.6	10.6	3
1406	868.4	18.5	10.6	4
1437	865.2	18.3	8.7	3
1468	862.1	18.1	9.0	3
1501	858.8	17.9	8.9	2

Table II - Sounding 2
(continued)

Height	Pressure	Temperature	Mixing Ratio	Turbulence
m	mb	°C	gm/kgm	Index
1533	855.6	17.6	8.1	1
1567	852.5	17.9	7.0	1
1605	849.2	17.6	7.2	2
1641	846.0	17.5	7.1	3
1674	843.0	17.3	6.8	2
1710	839.8	17.2	6.6	2
1746	836.7	16.8	6.3	2
1779	833.6	16.7	6.0	3
1813	830.5	16.6	5.7	2
1848	827.4	16.4	5.9	1
1884	824.3	16.1	5.6	2
1917	821.2	16.2	5.4	1
1950	818.2	16.0	5.2	1

Table III - Sounding 3 Over plains

1345 - 1415 LST

Height m	Pressure mb	Temperature °C	Mixing Ratio gm/kgm	Turbulence Index
320	984	25.9	18.0	21
355	980	25.8	18.1	58
385	977	25.3	18.0	55
420	973	24.9	18.3	51
448	970	24.8	17.3	48
485	966	24.5	17.7	44
510	963	24.3	17.9	38.5
545	959	24.4	17.7	31
575	956	23.8	17.5	25
610	952	23.3	17.5	32.5
635	949	23.0	17.1	38
670	945	22.6	17.1	30
705	942	22.7	16.3	27
740	938	22.7	16.6	24
765	935	22.7	15.6	30.5
795	932	22.5	16.5	38
830	928	21.4	15.1	26.5
860	925	21.0	16.1	17
900	921	20.6	16.3	9
925	918	20.8	15.2	10
955	915	21.0	14.1	11
990	911	20.5	14.6	10
1015	908	19.95	14.7	9.5

Table III - Sounding 3
(continued)

Height	Pressure	Temperature	Mixing Ratio	Turbulence
m	mb	°C	gm/kgm	Index
1045	905	20.5	13.2	9
1085	901	20.2	13.1	12
1115	898	19.85	13.2	14
1140	895	19.75	13.3	20
1185	891	19.65	13.4	22
1210	888	19.15	13.2	23
1240	885	19.05	13.8	18.5
1275	882	18.8	13.3	13
1310	878	18.2	12.5	11.5
1340	875	18.5	11.6	11
1370	872	18.4	12.2	13
1395	869	17.7	12.8	17
1435	865	18.1	11.5	19
1465	862	17.7	11.2	11
1495	859	17.2	11.3	13
1525	856	17.3	11.2	14
1555	853	17.2	10.6	12
1595	849	16.8	10.7	11
1625	846	16.5	10.8	4
1655	843	16.0	11.0	2
1690	840	16.2	10.6	13
1715	837	15.9	10.2	12
1750	834	15.9	9.6	5

Table III - Sounding 3
(continued)

Height	Pressure	Temperature	Mixing Ratio	Turbulence
m	mb	°C	gm/kgm	Index
1775	831	16.0	9.0	6
1810	828	15.1	10.2	7
1850	824	15.7	8.5	8
1880	821	14.6	10.2	4
1910	818	15.0	8.8	22
1940	815	14.2	9.5	24
1970	812	14.5	8.1	26
1995	809	14.6	8.0	23
2030	806	14.2	8.0	19
2070	803	13.7	8.0	36
2100	800	14.5	6.6	34
2135	797	14.1	6.8	28
2170	794	14.2	6.4	22
2205	791	14.4	5.3	18
2240	788	13.2	6.1	43

Table IV - Sounding 4 Off lee shore

1510 - 1600 LST

Height	Pressure	Temperature	Mixing Ratio	Turbulence
m	mb	°C	gm/kgm	Index
20	1018	28.3	18.6	10
35	1016	28.1	18.7	11
65	1013	27.5	18.4	12.5
95	1009	27.3	18.2	14
135	1005	27.2	18.0	16
159	1002	26.9	18.1	17
192	998	26.6	17.3	10
220	995	26.6	16.3	9
255	991	26.2	17.3	8
290	987	26.5	15.3	4
320	984	26.2	15.1	4
355	980	24.7	18.2	9
387	977	25.1	16.1	6
420	973	25.1	15.8	4
445	970	24.5	16.2	3
485	966	24.4	15.8	3
510	963	24.0	16.0	3
545	959	23.7	16.0	4
580	956	24.8	14.1	5
610	952	24.3	14.4	5
635	949	23.9	14.6	4
700	942	23.9	13.8	4
740	938	24.0	13.6	3

Table IV - Sounding 4
(continued)

Height	Pressure	Temperature	Mixing Ratio	Turbulence
m	mb	°C	gm/kgm	Index
770	935	23.9	13.2	3
795	932	23.6	13.5	2
835	928	23.4	13.5	3
860	925	23.3	13.4	3
900	921	23.1	13.0	4
925	918	23.1	12.6	4
955	915	23.0	12.2	4
995	911	22.8	12.2	6
1020	908	22.5	11.6	7
1050	905	22.4	11.8	7
1090	901	22.0	11.6	4
1115	898	21.7	11.4	6
1145	895	21.4	11.1	6
1182	891	21.3	11.0	5
1210	888	20.8	10.8	5.5
1240	885	20.6	10.8	5
1270	882	20.3	10.9	5
1308	878	20.0	10.7	5
1338	875	19.9	11.0	4.5
1370	872	19.6	11.1	4
1395	869	18.2	12.1	4
1435	865	18.4	12.6	6
1465	862	18.4	12.0	7

Table IV - Sounding 4
(continued)

Height	Pressure	Temperature	Mixing Ratio	Turbulence
m	mb	°C	gm/kgm	Index
1495	859	18.3	11.2	7
1530	856	18.1	10.6	5
1555	853	17.6	11.2	6
1595	849	17.6	11.0	4
1625	846	17.3	11.2	4.5
1655	843	16.4	11.6	5
1685	840	16.4	11.1	7
1720	837	16.4	11.0	7
1748	834	16.1	11.0	8
1775	831	15.5	11.3	6
1808	828	15.1	11.0	7
1850	824	15.5	10.0	3
1880	821	15.1	10.3	4
1910	818	14.8	9.9	3
1945	815	14.6	10.0	3
1973	812	14.4	9.7	3
2005	809	14.4	8.7	3
2040	806	14.2	9.9	3
2070	803	14.0	10.0	3
2100	800	14.2	9.7	2
2135	797	14.0	9.5	4
2170	794	13.8	9.4	4
2200	791	13.4	9.4	4

Table IV - Sounding 4
(continued)

Height	Pressure	Temperature	Mixing Ratio	Turbulence
m	mb	°C	gm/kgm	Index
2238	788	13.3	9.0	3
2270	785	13.0	9.4	2
2305	782	12.6	9.7	2
2325	780	12.6	8.4	3
2355	777	12.4	8.2	3
2385	774	12.4	7.8	3
2410	771	12.4	7.3	3
2435	768	12.3	5.6	3
2455	765	12.6	4.9	2
2487	762	12.6	4.7	3
2512	759	12.3	4.5	3
2535	756	12.3	4.4	2
2560	753	11.7	4.9	3
2585	750	11.5	4.6	

LOCATIONS OF SOUNDINGS AND PHOTOGRAPHS OVER PUERTO RICO
NEAR NOON – JUNE 25 1952

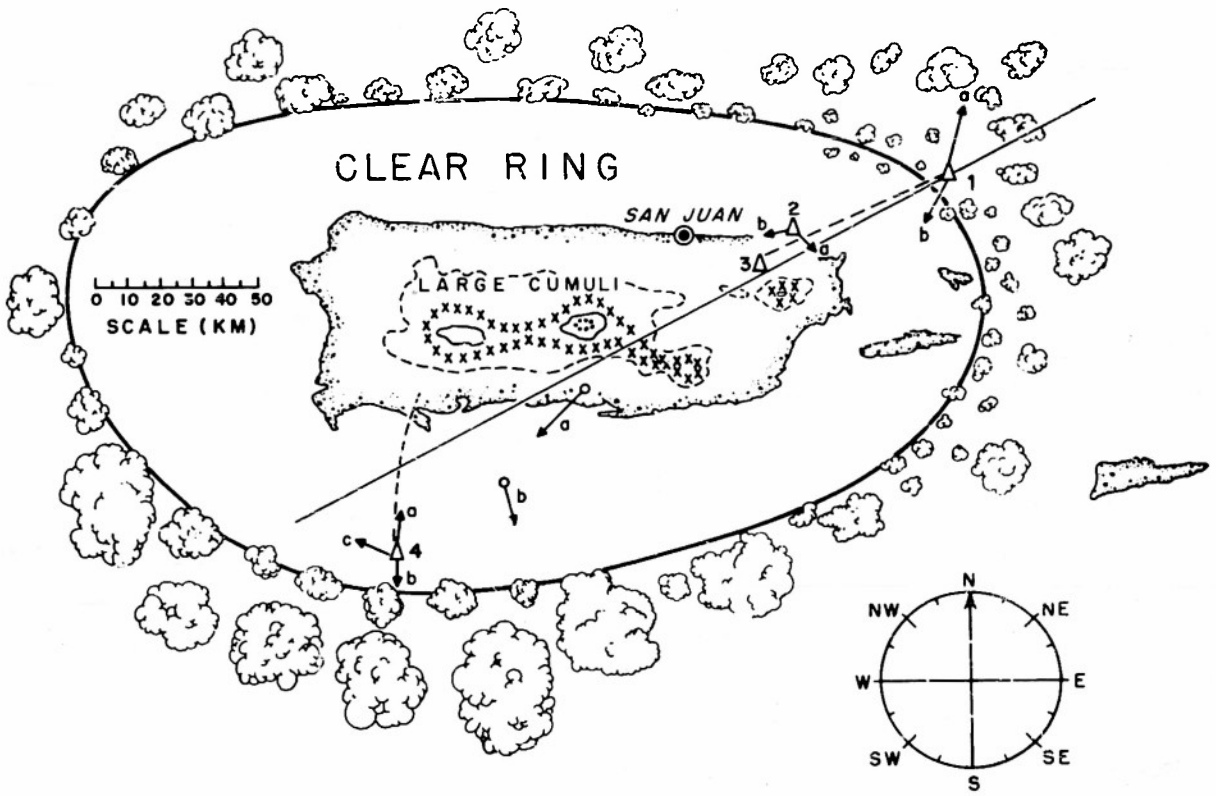

FIG. 1

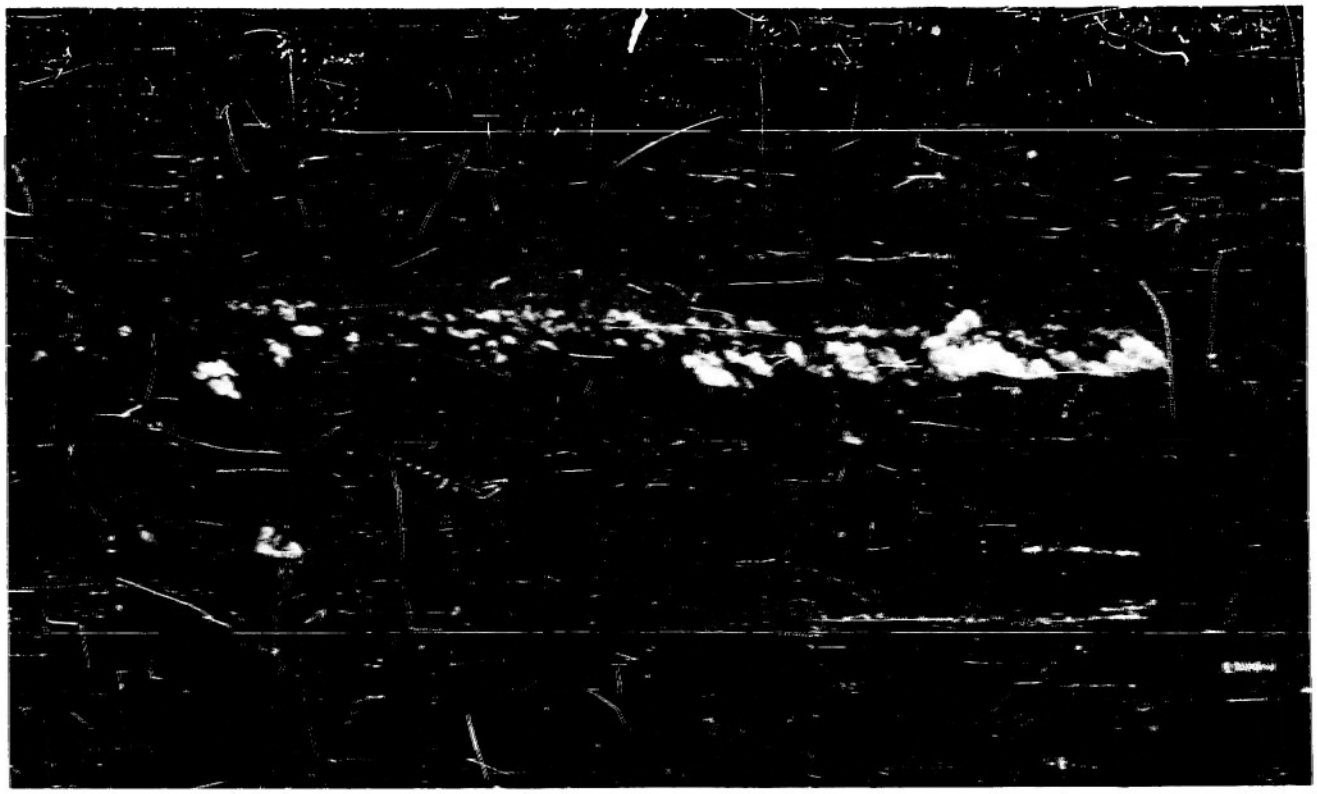

A

B

FIG. 2

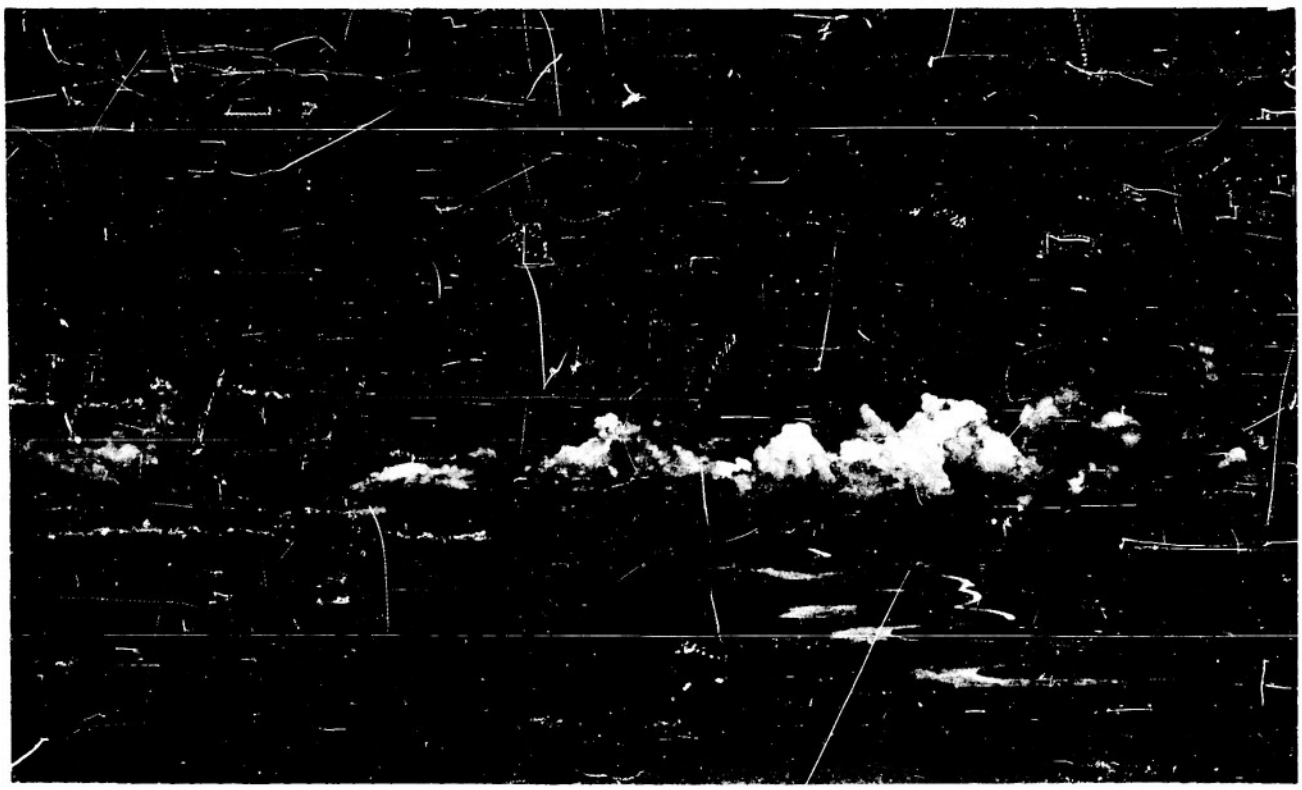

A

B

FIG. 3

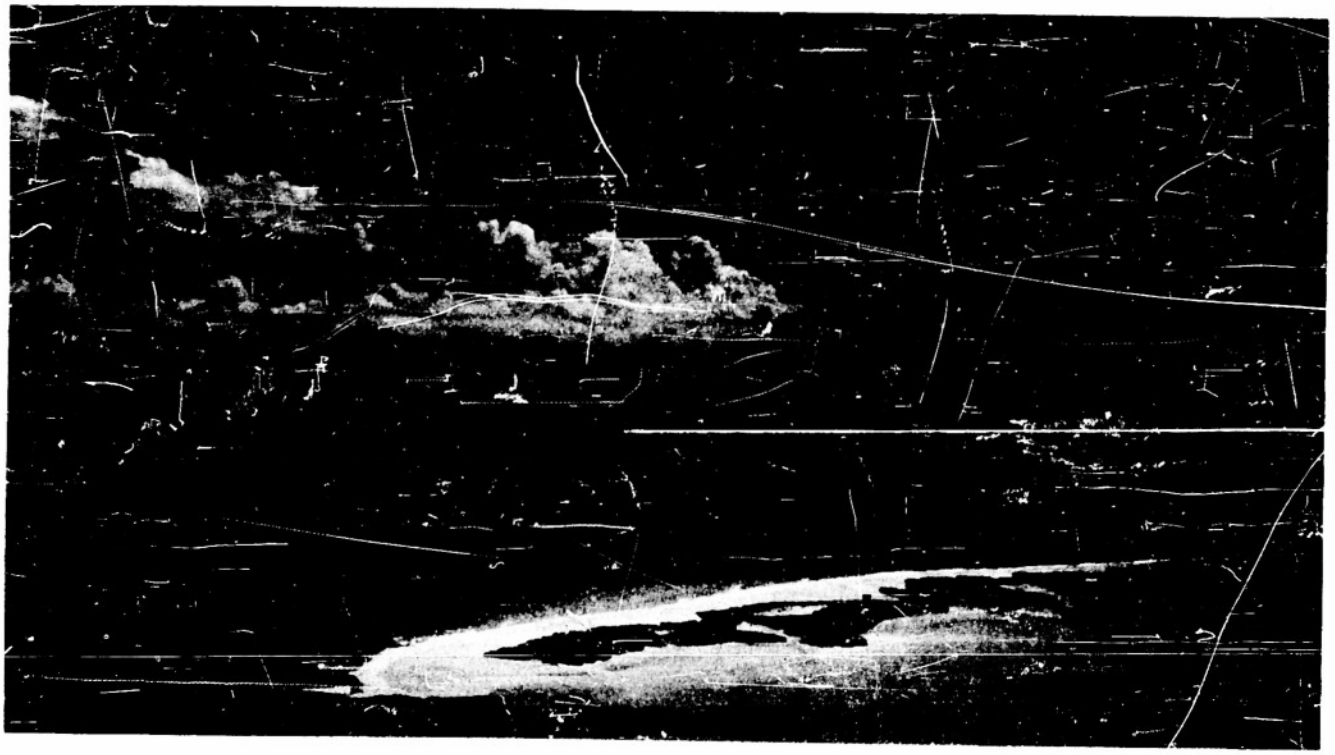

A

B

FIG. 4

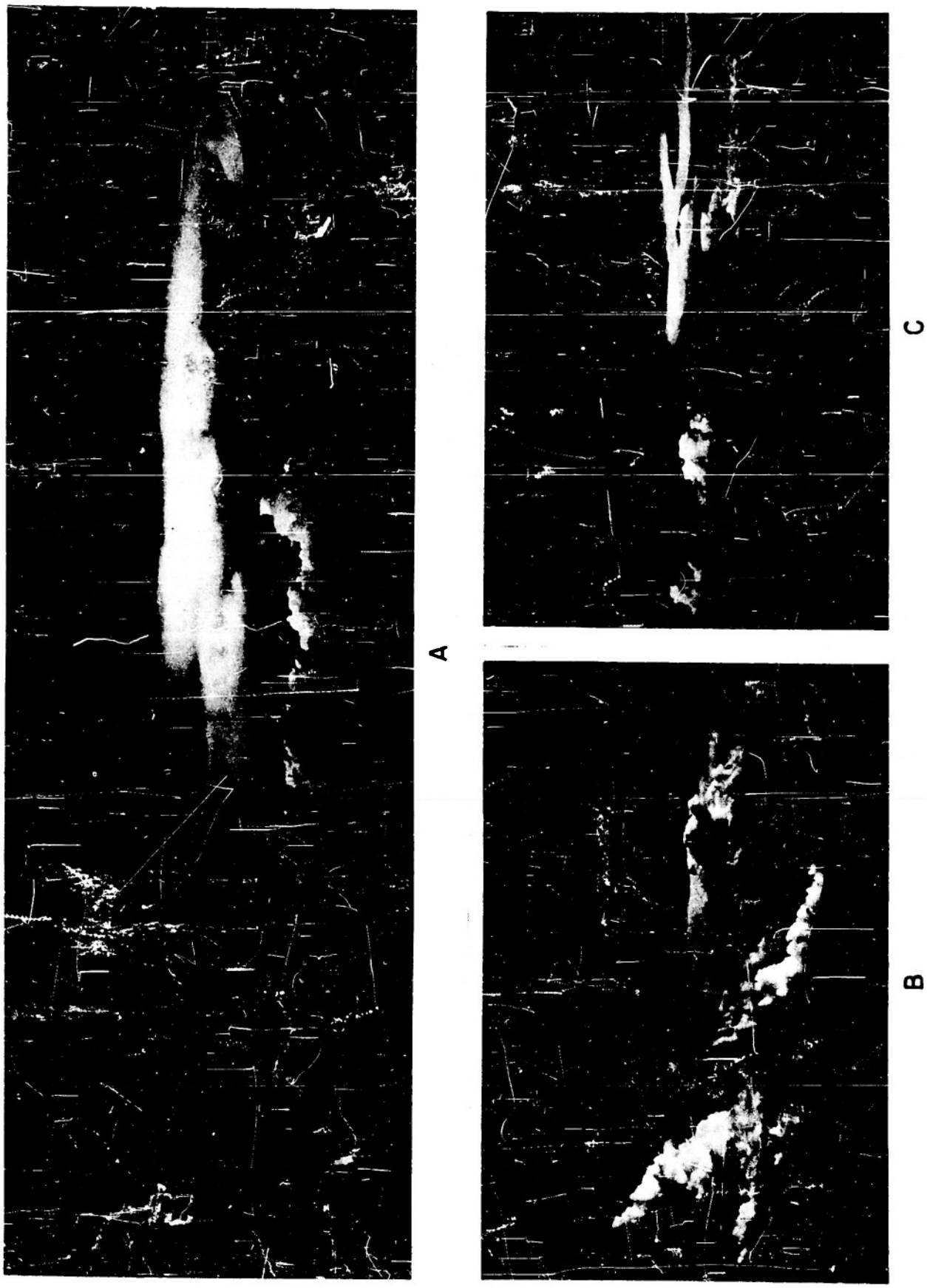

FIG. 5

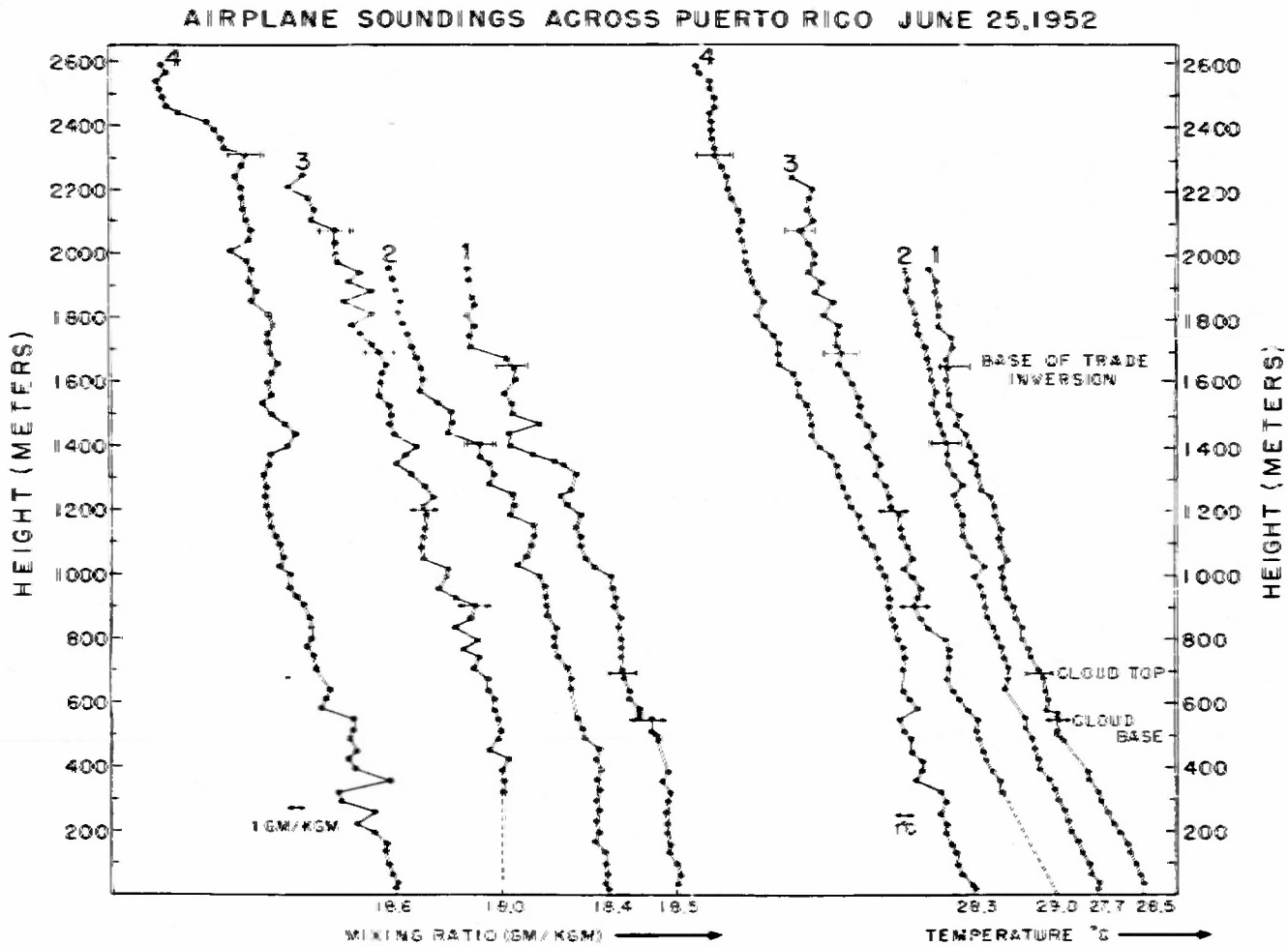
AIRPLANE SOUNDINGS ACROSS PUERTO RICO JUNE 25,1952
HEIGHT (METERS)
2600
2400
2200
2000
1800
1600
1400
1200
1000
800
600
400
200
4
3
2
1
1 GM/KGM
18.6
19.0
18.4
18.5
MIXING RATIO (GM/KGM)
28.3
29.0
27.7
28.5
TEMPERATURE °C
BASE OF TRADE INVERSION
CLOUD TOP
CLOUD BASE

FIG. 6

POTENTIAL TEMPERATURE (°A)——
MIXING RATIO (GM/KGM)------

OVER PUERTO RICO
NEAR NOON – JUNE 25 1952

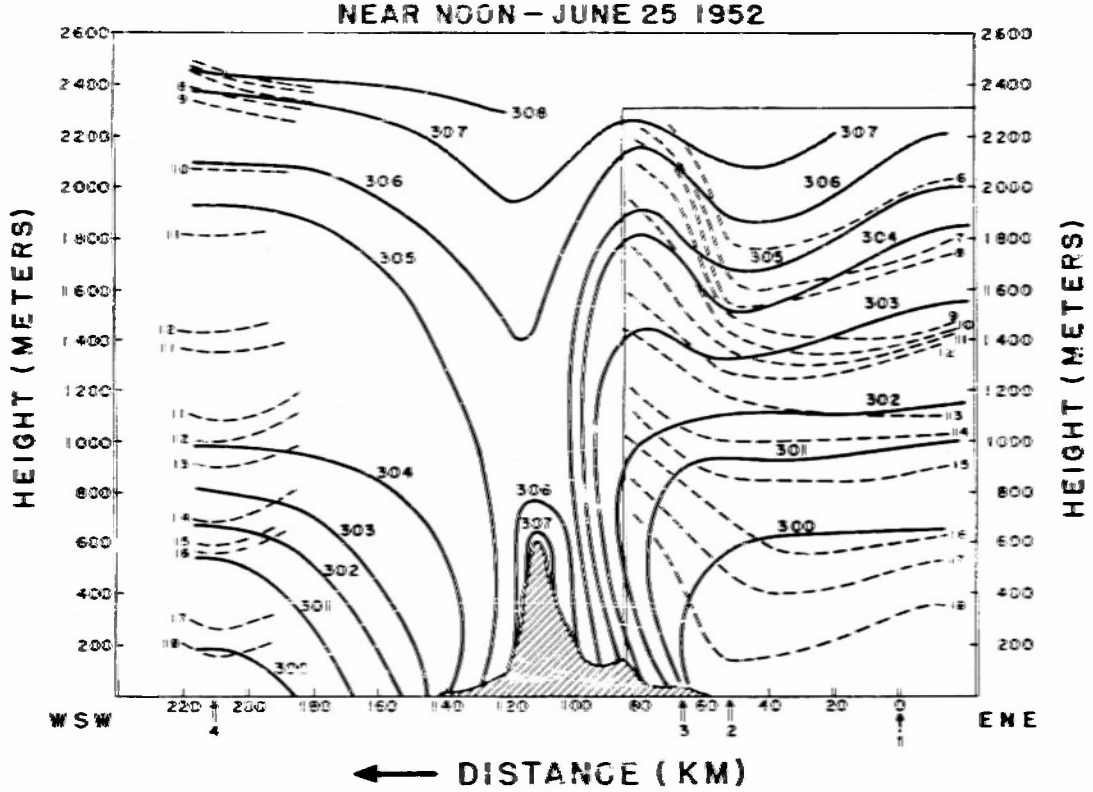

FIG.7

CLOUD, STABILITY, AND WIND STRUCTURE
OVER PUERTO RICO
NEAR NOON – JUNE 25 1952

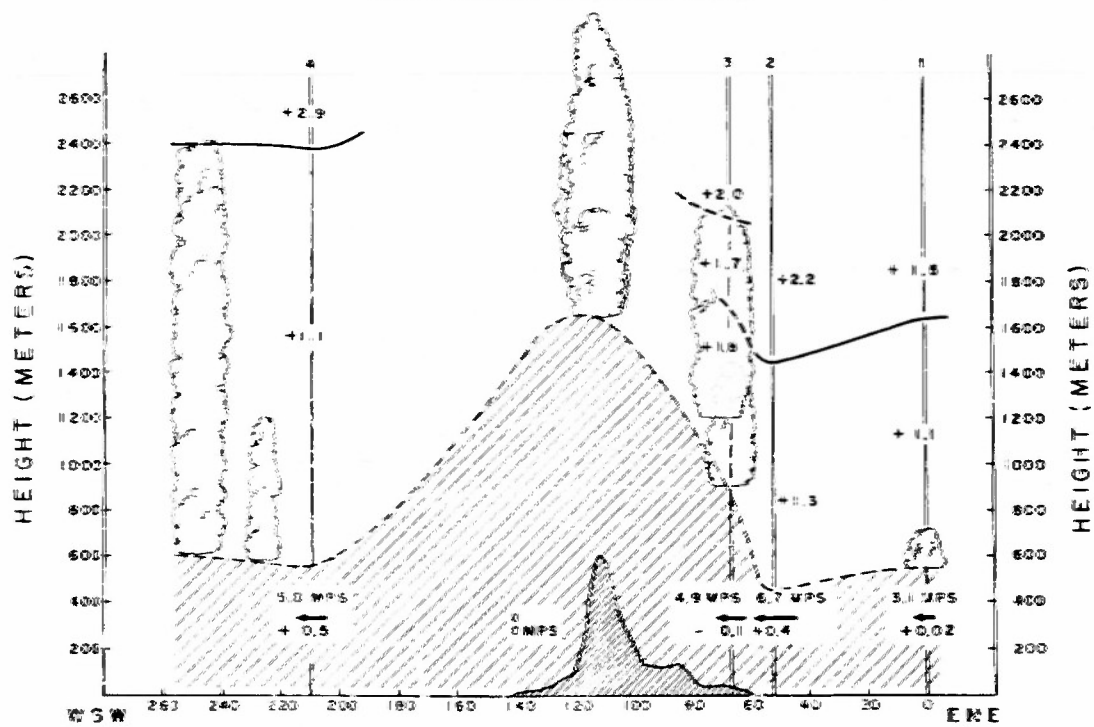

FIG.8

CALCULATED AIR FLOW OVER PUERTO RICO
NEAR NOON - JUNE 25, 1952
——— TOTAL STREAMLINES
------ PERTURBATION STREAMLINES

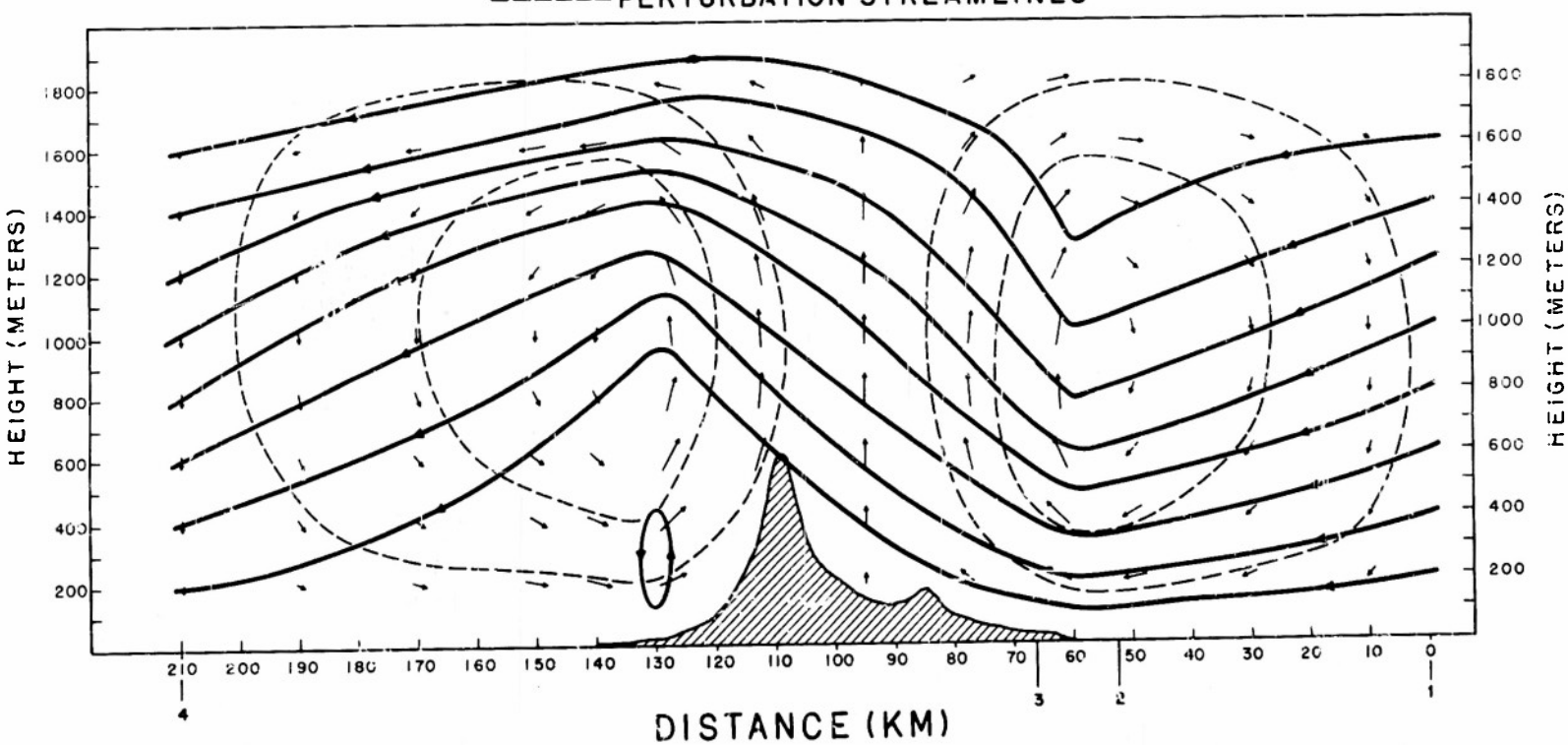

FIG. 9

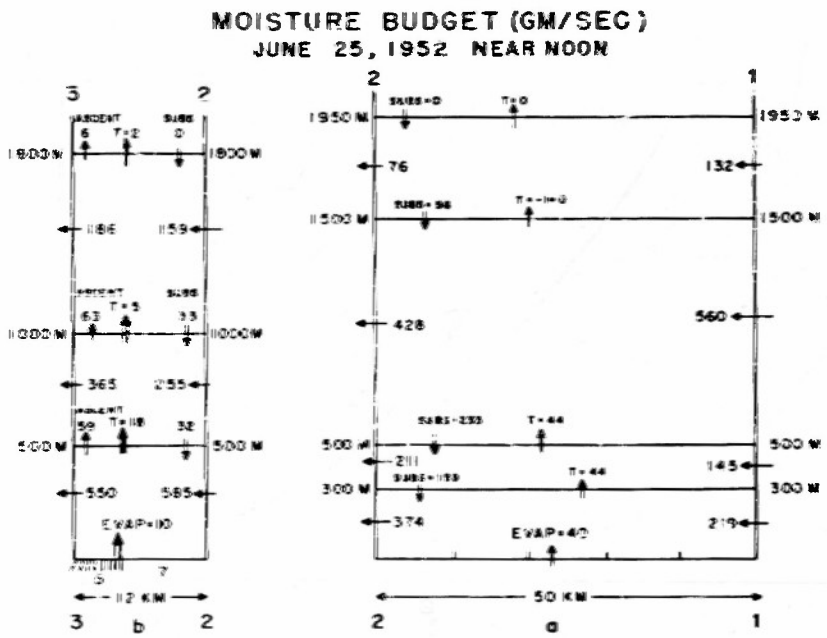
MOISTURE BUDGET (GM/SEC)
JUNE 25, 1952 NEAR NOON
3
2
1900 M
1800 M
1186
1159
1000 M
365
255
500 M
550
585
EWAP=10
12 KM
3
b
2
1950 M
1500 M
76
132
428
560
500 M
211
145
300 M
374
219
EWAP=40
50 KM
2
a
1

FIG.10

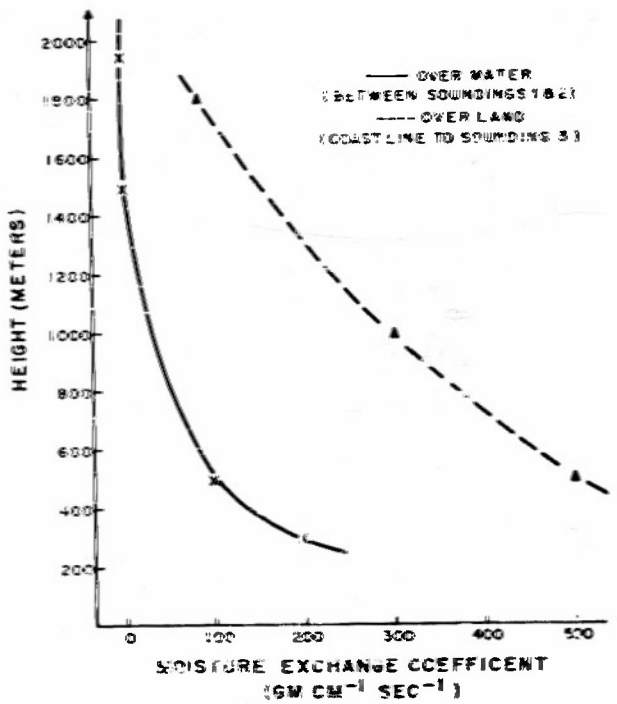
OVER WATER
(BETWEEN SOUNDINGS 1 & 2)
OVER LAND
(COAST LINE TO SOUNDING 3)
HEIGHT (METERS)
2000
1800
1600
1400
1200
1000
800
600
400
200
0
100
200
300
400
500
MOISTURE EXCHANGE COEFFICENT
(GM CM⁻¹ SEC⁻¹)

FIG.11

Technical Report Distribution List
ONR Project NR-082-021

24 August 1953

Addressee	Copies
Geophysics Branch, Code 416, Office of Naval Research Washington 25, D. C.	2
Director, Naval Research Laboratory, Attention: Technical Information Officer, Washington 25, D. C.	6
Officer-in-Charge, Office of Naval Research London Branch Office, Navy No. 100, Fleet Post Office, New York, New York	2
Office of Naval Research Branch Office, 346 Broadway, New York 13, New York	1
Office of Naval Research Branch Office, 150 Causeway Street, Boston, Massachusetts	1
Office of Naval Research Branch Office, Tenth Floor, The John Crerar Library Building, 86 East Randolph Street, Chicago, Illinois	1
Office of Naval Research Branch Office, 1030 East Green Street, Pasadena 1, California	1
Office of Naval Research Branch Office, 1000 Geary Street, San Francisco, California	1
Office of Technical Services, Department of Commerce, Washington 25, D. C.	1
Armed Services Technical Information Center, Documents Service Center, Knott Building, Dayton 2, Ohio	5
Assistant Secretary of Defense for Research and Development, Attn: Committee on Geophysics and Geography, Pentagon Building, Washington 25, D. C.	1
Department of Aerology, U. S. Naval Post Graduate School, Monterey, California	1
Aerology Branch, Bureau of Aeronautics (Ma-5), Navy Department, Washington 25, D. C.	1
Mechanics Division, Naval Research Laboratory, Anacostia Station, Washington 20, D. C., Attention: J. E. Dinger, Code 3820	1

Addressee	Copies
Radio Division I, Code 3420, Naval Research Laboratory, Anacostia Station, Washington 20, D. C.	1
Meteorology Section, Navy Electronics Laboratory, San Diego 52, California, Attention: L. J. Anderson	1
Library, Naval Ordnance Laboratory, White Oak, Silver Spring 19, Maryland	1
Bureau of Ships, Navy Department, Washington 25, D. C., Attention: Code 851 (Special Devices Center)	1
Bureau of Ships, Navy Department, Washington 25, D. C., Attention: Code 327 (Technical Library)	2
Chief of Naval Operations, Navy Department, Washington 25, D. C., Attention: Op-533D	2
Oceanographic Division, U. S. Navy Hydrographic Office, Suitland, Maryland	1
Library, Naval Ordnance Test Station, Inyokern, China Lake, California	1
Project Arowa, U. S. Naval Air Station, Building R-48, Norfolk, Virginia	2
The Chief, Armed Forces Special Weapons Project, P. O. Box 2610, Washington, D. C.	1
Office of the Chief Signal Officer, Engineering and Technical Service, Washington 25, D. C., Attn: SIGGGM	1
Meteorological Branch, Evans Signal Laboratory, Belmar, New Jersey	1
Headquarters Quartermaster Research and Development Command. Quartermaster Research and Development Center, U. S. Army, Natick, Massachusetts. Attention: Environmental Protection Division	1
Office of the Chief, Chemical Corps, Research and Engineering Division, Research Branch, Army Chemical Center, Maryland	2

Addressee	Copies
Commanding Officer, Air Force Cambridge Research Center, 230 Albany Street, Cambridge, Massachusetts, Attention: ERHS-1	1
Headquarters, Air Weather Service, Andrews Air Force Base, Washington 20, D. C., Attention: Director Scientific Services	2
Commanding General, Air Materiel Command, Wright Field, Dayton, Ohio, Attention: MCREEO	1
Commanding General, Air Force Cambridge Research Center, 230 Albany Street, Cambridge, Massachusetts, Attention: CRHSL	1
Commanding General, Air Research and Development Command, P. O. Box 1395, Baltimore 3, Maryland	1
Department of Meteorology, Massachusetts Institute of Technology, Cambridge, Massachusetts, Attention: H. G. Houghton	1
Department of Meteorology, University of Chicago, Chicago 37, Illinois, Attention: H. R. Byers	1
Institute for Advanced Study, Princeton, New Jersey, Attention: J. von Neumann	1
Scripps Institution of Oceanography, La Jolla, California Attention: R. Revelle	1
General Electric Research Laboratory, Schenectady, New York, Attention: I. Langmuir	1
St. Louis University, 3621 Olive Street, St. Louis 8, Missouri, Attention: J. B. Macelwane, S. J.	1
Department of Meteorology, University of California at Los Angeles, Los Angeles, California, Attention: M. Neiburger	1
Department of Engineering, University of California at Los Angeles, Los Angeles, California, Attention: L. M. K. Boelter	1

Addressee	Copies
Department of Meteorology, Florida State University, Tallahassee, Florida, Attention: W. A. Baum	1
Woods Hole Oceanographic Institution, Woods Hole. Massachusetts, Attention: C. Iselin	1
The Johns Hopkins University, Department of Civil Engineering, Baltimore, Maryland, Attention: R. Long	1
The Johns Hopkins University, Department of Physics, Homewood Campus, Baltimore, Maryland, Attention: G. Plass	1
New Mexico Institute of Mining and Technology, Research and Development Division, Socorro, New Mexico, Attention: E. Workman	1
University of Chicago, Department of Meteorology, Chicago 37, Illinois, Attention: H. Riehl	1
Woods Hole Oceanographic Institution, Woods Hole, Massachusetts, Attention: A. Woodcock	1
General Electric Research Laboratory, Schenectady, New York, Attention: V. Schaefer	1
Geophysical Institute, University of Alaska, College, Alaska, Attention: C. T. Elvey	1
Blue Hill Meteorological Observatory, Harvard University, Milton 86, Massachusetts, Attention: C. Brooks	1
Laboratory of Climatology, Johns Hopkins University, Seabrook, New Jersey	1
Department of Meteorology, New York University, New York 53, New York, Attention: B. Haurwitz	1
Texas A and M, Department of Oceanography. College Station, Texas, Attention: J. Freeman. Jr.	1
Massachusetts Institute of Technology, Department of Meteorology, 77 Massachusetts Avenue, Cambridge 39, Massachusetts, Attention: T. F. Malone	1

Addressee	Copies
Rutgers University, College of Agriculture, Department of Meteorology, New Brunswick, New Jersey	1
National Advisory Committee of Aeronautics, 1500 New Hampshire Avenue, N. W., Washington 25, D. C.	2
U. S. Weather Bureau, 24th and M Streets, N. W., Washington 25, D. C., Attention: Scientific Services Division	2
Air Coordinating Committee, Subcommittee on Aviation Meteorology, Room 2D889-A, The Pentagon, Washington, D. C.	1
American Meteorological Society, 3 Joy Street, Boston 8, Massachusetts, Attention: The Executive Secretary	1
Research Professor of Aerological Engineering, College of Engineering, Department of Electrical Engineering, University of Florida, Gainesville, Florida	1
The Hydrographer, U. S. Navy Hydrographic Office, Washington 25, D. C.	8

ADDITIONAL DISTRIBUTION LIST

Addressee	Copies
Brookhaven National Laboratory, Upton, L. I., New York, Attention: Meteorology Group	1
Chemical Corps, Biological Laboratories, Technical Library, Camp Detrick, Frederick, Maryland	2
Dr. August Raspet, Engineering and Industrial Research Station, Mississippi State College, State College, Mississippi	2
Dr. E. W. Hewson, Diffusion Project, Round Hill, South Dartmouth, Massachusetts	1
Dr. Hunter Rouse, Director, Iowa Institute of Hydraulic Research, State University of Iowa, Iowa City, Iowa	1

Addressee	Copies
Head, Department of Physics, University of New Mexico, Albuquerque, New Mexico	1
Mr. Wendell A. Mordy, Hawaiian Pineapple Research Institute, Honolulu, Hawaii	1
Dr. E. G. Bowen, Chief, Division of Radiophysics, Commonwealth Scientific Industrial Research Organization, University Grounds, Chippendale, N. S. W., Australia	1
Professor Max A. Woodbury, Department of Statistics, Wharton School, University of Pennsylvania, Philadelphia 4, Pennsylvania	1
Pennsylvania State College, School of Mineral Industries, State College, Pennsylvania, Attention: H. Panofsky	1
University of Wisconsin, Department of Meteorology, Madison, Wisconsin, Attention: V. Suomi	1